Rapid Information Transfer in Swarms Under Update-Rate-Bounds Using Delayed Self-Reinforcement

Santosh Devasia

Fellow ASME
Mechanical Engineering Department,
University of Washington,
Seattle, WA 98195-2600
e-mail: devasia@uw.edu

The effectiveness of a network's response to external stimuli depends on rapid distortion-free information transfer across the network. However, the rate of information transfer, when each agent aligns with information from its network neighbors, is limited by the update rate at which each individual can sense and process information. Moreover, such neighbor-based, diffusion-type information transfer does not predict the superfluid-like information transfer during swarming maneuvers observed in nature. The main contribution of this paper is to propose a novel model that uses self-reinforcement, where each individual augments its neighbor-averaged information update using its previous update to (i) increase the information-transfer rate without requiring an increased, individual update-rate and (ii) enable superfluid-like information transfer. Simulations results of example systems show substantial improvement, more than an order of magnitude increase, in the information transfer rate, without the need to increase the update rate. Moreover, the results show that the delayed self-reinforcement (DSR) approach's ability to enable superfluid-like, distortion-free information transfer results in maneuvers with smaller turn radius and improved cohesiveness. Such faster response rate with limited individual update rate can enable better understanding of cohesiveness of flocking in nature, as well as improve the performance of engineered swarms such as unmanned mobile systems. [DOI: 10.1115/1.4042949]

1 Introduction

The information-transfer speed across the network impacts the effectiveness of a network's response to external stimuli. Aligning with neighbors in a network can model a range of problems such as control of autonomous mobile agents [1], distributed sensing [2], and particle and flocking dynamics, e.g., see Refs. [3–11]. Note that faster information transfer can be achieved by increasing the alignment strength, i.e., by scaling up the individual agent's update that is based on information from neighbors. Nevertheless, such an increase in the alignment strength will require an increase in the information-update rate at which each individual agent obtains information from other agents connected through the network and changes its own state. Bounds on the update rate can arise due to the time needed for each individual agent to sense, e.g., the time needed for an ultrasound sensor to ping and measure distance to a neighbor, and process information, e.g., the time needed for communication and computation. Hence, there is a limit to the maximum rate of information transfer possible with a given bound on the update rate.

Alternatively, instead of changing the alignment strength, the network connectivity could be optimized for fast response, e.g., see Refs. [12] and [13]. Nevertheless, the network response can be slow if the number of agent interconnections is small compared to the number of agents [14]. Previous works have studied convergence of response under time-varying connectivity, e.g., see Ref. [15], and shown that time-varying connections, such as randomized interconnections, can lead to faster response, e.g., see Ref. [14]. Another approach is to sequence the update of the agents to improve the response [16]. When such time-variations in the network connectivity are not feasible, i.e., for a given network connectivity, the need to maintain stability (based on the update rate) tends to limit the range of acceptable alignment strength, and therefore, limits the response rate. This motivates the need for new approaches to improve the response rate when the update rate is fixed. The main contribution of this paper is to propose a novel model that uses self-reinforcement to increase the information-transfer rate without the need to change the network structure or the bandwidth (information-update rate) of the individual agents. Rather, the proposed approach uses delayed versions of the previous updates from the network to self-reinforce the current update and improve the overall network response. Similar use of prior update has been used to improve the convergence of gradient-based search algorithms, e.g., in neural networks [17,18]. In the current article, it is shown the faster response rate can be achieved without increasing the individual update rate. Such increase in performance can enable better understanding of cohesiveness of flocking in nature, e.g., see Refs. [5] and [9], as well as improve the response of engineered swarms [19–21].

The current investigation on improved performance under constraints on the update rate is different from studies that seek to ensure convergence under say communication delays [22–25] or communication channel dynamics and resource constraints [26–28], which do not necessarily place bounds on the update rate, but needs to be considered when investigating stability. Previous works have also investigated the minimal data rate needed to ensure stability in terms of the quantization of information transferred during each update [29]. Although, such information communication rates are not considered in this paper, such criteria need to be met within the time between updates.

Another challenge with the current models of the neighbor-averaged diffusive information transfer is that they do not predict the superfluid-like information transfer observed in biological flocking [9,30]. Superfluid-like information transfer tends to have a linear propagation of the information with respect to time as opposed to a square-root-type dependence on time with standard

diffusion-type models, e.g., see Refs. [3–5]. More importantly, superfluid-like information transfer leads to undamped propagation of the radial acceleration across the flock, which is important to achieve equal-radius (parallel) trajectories for cohesive maneuvers [9]. Nevertheless, superfluid-like models also require an increase in update rate for fast response. This paper shows that the current diffusive models can be modified using the delayed self-reinforcement to capture the superfluid-like information transfer observed in nature without the need to increase the update rate of the individual agents.

The paper begins with the response-speed limitations of current standard diffusion-based models and then presents the proposed delayed self-reinforcement approach in Sec. 2. Simulations are presented in Sec. 3 to comparatively evaluate the performance improvement with and without delayed self-reinforcement (DSR) and to clarify the impact on cohesiveness of a swarm during turn maneuvers. This is followed by the conclusions in Sec. 4.

2 Delayed Self-Reinforcement Approach

This section begins by describing the standard diffusion-based information transfer model without the DSR. The response-speed limitation with such models is described, followed by a presentation of the proposed DSR approach and an analysis of the DSR-based model's ability to capture superfluid-like information transfer.

2.1 Information Transfer Without Delayed Self-Reinforcement. The standard, diffusion-based, information-update model can be described by, e.g., see Refs. [3] and [4]

$$I_i(k+1) = I_i(k) - \gamma \Delta_i(k) \delta_t \qquad (1)$$

where $I_i(k)$ is the information state for the ith individual in the swarm and different integers k represent the update time instants

$$t_k = k \delta_t \qquad (2)$$

the fixed time interval between updates is δ_t, γ is the alignment strength, and $\Delta_i(k)$ is the average difference in the information between the individual and agents from the set of neighbors N_i

$$\Delta_i(k) = \frac{1}{|N_i|} \sum_{j \in N_i} \left[I_i(k) - I_j(k) \right] \quad \text{if } |N_i| \neq 0$$
$$= 0 \quad \text{otherwise} \qquad (3)$$

where $|N_i|$ is the number of neighbors in the set N_i. In the current model, the set of neighbors N_i also includes the virtual, information-source agent s when the individual i is a leader with direct access to the source information I_s.

Remark 1 (Selection of neighbors). The information I_i of each agent i is updated in Eq. (1) based on the information available from its neighbors N_i. In typical flocking models, the neighbors of an agent have been selected based on different criteria such as (i) the field of view of each agent, (ii) the metric distance between agents as well as (iii) the topological distance between agents, e.g., see Refs. [4], [5], and [31].

2.2 Response-Speed Limit. Studies of starling flocks have shown that the propagation of orientation changes (and the corresponding information transfer) among agents can be fast compared to spatial reorganization of the agents with respect to each other [9]. Therefore, the information dynamics in Eq. (1) can be rewritten, for short periods of time around any time instant t_k, without considering reorganization of agents relative to each other, as

$$I(k+1) = I(k) - \gamma A \delta_t I(k) + \gamma B \delta_t I_s(k) \qquad (4)$$

where the matrices A and B are given by

$$A(i,j) = -1/|N_i| \quad \text{if } j \in N_i, \text{ and } j \neq i$$
$$= 1 \qquad \text{if } j = i \text{ and } |N_i| \neq 0$$
$$= 0 \qquad \text{otherwise} \qquad (5)$$
$$B(i) = 1/|N_i| \quad \text{if } s \in N_i$$
$$= 0 \qquad \text{otherwise}$$

The continuous-time version of the approximated dynamics in Eq. (4) is

$$\frac{d}{dt} I(t) = -\gamma A I(t) + \gamma B I_s(t) \qquad (6)$$

Stability of the continuous-time dynamics in Eq. (6) can be inferred through the graph representing the neighbor-based connectivity of the agents. In particular, let the neighbor-based connectivity of the agents be represented by a directed graph (digraph) $\mathcal{G} = (\mathcal{V}, \mathcal{E})$, e.g., as defined in Ref. [22], with agents represented by nodes $\mathcal{V} = \{1, 2, \ldots, n, s\}$, $n > 1$ and edges $\mathcal{E} \subseteq \mathcal{V} \times \mathcal{V}$, where each agent j in the set of neighbors $N_i \subseteq \mathcal{V}$ of the agent i satisfies $j \neq i$ with an associated edge $(j, i) \in \mathcal{E}$. If all agents have access to the virtual-source agent's state I_s through the graph, i.e., there is a directed path from the source node s to any node $i \in \mathcal{V} \setminus s$, then A is Hurwitz, i.e., the eigenvalues λ_A of matrix A lie in the open-left half of the complex plane, e.g., see Ref. [32]. Moreover, when the information source I_s is a fixed value, consensus is reached asymptotically, and the information state I of all agents approach the information source I_s, i.e., $\lim_{t \to \infty} I_i(t) = I_s$ for all agents i.

The response speed of the continuous-time dynamics in Eq. (6) increases with alignment strength γ when there is a directed path from the source node s to all agents $i \in \mathcal{V} \setminus s$. This follows since the poles λ_c of the continuous-time system in Eq. (6)

$$\lambda_c = \gamma \lambda_A \qquad (7)$$

move away (toward the left) from the imaginary axis as the alignment strength γ is increased.

There is a limit to the achievable increase in response speed of the diffusion-based, information transfer in Eq. (1) by increasing the alignment strength γ for a fixed update rate, i.e., a fixed update-time interval δ_t. Note that the increased response speed with increases in the alignment strength γ of the continuous-time dynamics in Eq. (6) also results in an increase in the response speed of the corresponding discrete-time dynamics in Eq. (4), provided the update-time interval δ_t is sufficiently small. Therefore, the response speed of the diffusion-based, information-update dynamics in Eq. (1) also increases with the alignment strength γ. Nevertheless, for a fixed update-time interval δ_t, the discrete-time dynamics in Eq. (4) can become unstable for large values of the alignment strength γ. In particular, the poles λ_d of the discrete-time system in Eq. (4), given by

$$\lambda_d = 1 - \delta_t \lambda_c = 1 - \delta_t \gamma \lambda_A \qquad (8)$$

can become larger than one in magnitude ($|\lambda_d| > 1$) if the alignment strength γ is sufficiently large. Thus, the need to maintain stability, i.e., for each eigenvalue λ_A

$$|1 - \delta_t \gamma \lambda_A| < 1 \qquad (9)$$

limits the maximum acceptable value of the alignment strength γ when the update rate δ_t is fixed, and therefore, limits the potential to increase the response speed of diffusion-based information transfer.

2.3 Proposed Information Transfer With Delayed Self-Reinforcement. Let the information update $[I_i(k+1) - I_i(k)]$ be reinforced by the previous update, $[I_i(k) - I_i(k-1)]$, as

$$[I_i(k+1) - I_i(k)] = -\gamma \Delta_i(k)\delta_t + \beta[I_i(k) - I_i(k-1)] \qquad (10)$$

where β is the DSR gain on the previous update, $[I_i(k) - I_i(k-1)]$. This leads to the following modified information-update model:

$$I_i(k+1) = I_i(k) - \gamma \Delta_i(k)\delta_t + \beta[I_i(k) - I_i(k-1)] \qquad (11)$$

which is illustrated in Fig. 1.

Remark 2 (DSR and no-DSR models). Note that if the DSR gain β in Eq. (11) is set to zero, then it reduces to the standard diffusion-based, information-update model in Eq. (1).

Remark 3 (Information to implement DSR). Implementing the DSR does not require additional information from the neighbors. Rather, the self-reinforcement approach requires each agent to store a delayed version $I_i(k-1)$ of its current state $I_i(k)$ and to have knowledge of the DSR gain β as illustrated in Fig. 1.

2.4 Superfluid-Type Information Transfer. To understand the impact of the DSR gain β selection on capturing the superfluid-like behavior, let the information update in Eq. (11) be first rewritten as

$$\frac{\beta}{\delta_t}\left\{[I_i(k+1) - I_i(k)] - [I_i(k) - I_i(k-1)]\right\}$$
$$+ \frac{1-\beta}{\delta_t}[I_i(k+1) - I_i(k)] = -\gamma \Delta_i(k) \qquad (12)$$

The above equation can then be approximated by the damped-wave equation, when the update-time interval δ_t is small compared to the information-transfer response, as

$$\beta \delta_t \frac{\partial^2}{\partial t^2}I(t,X) + (1-\beta)\frac{\partial}{\partial t}I(t,X) = \gamma \frac{a^2}{2D}\nabla^2 I(t,X) \qquad (13)$$

where a is the average distance to the neighbors, X represents the spatial location of agents, D is the number of dimensions of the spatial variable X over which the information I is varying, and ∇^2 represents the Laplacian.

Remark 4 (Laplacian approximation). The Laplacian is approximated in Eq. (13) using the average difference $\Delta_i(k)$, e.g., as in Ref. [9]

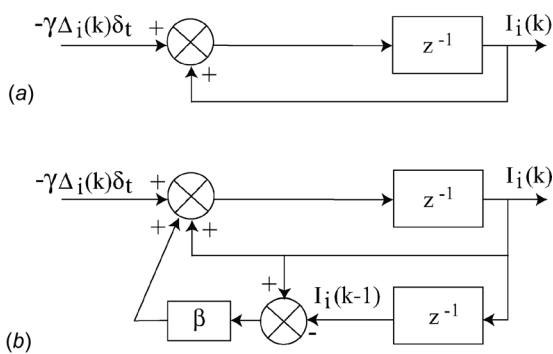$$\nabla^2 I(t,X) \approx -\frac{2D}{a^2}\Delta_i(k) \qquad (14)$$

(a)

(b)

Fig. 1 Control implementation with and without DSR: (a) dynamics of agent *i* without delayed self-reinforcement (DSR) and (b) modified dynamics of agent *i* with DSR, which does not need additional information from other agents

Note that along each dimension, say the x dimension with an associated unit vector $\hat{x}$, the second partial derivative

$$\frac{\partial^2}{\partial x^2}I(t,X) \approx \frac{1}{a^2}\left[I(t,X+a\hat{x}) - 2I(t,X) + I(t,X-a\hat{x})\right]$$
$$= -\frac{2}{a^2}\Delta_x \qquad (15)$$

is proportional to twice the average difference Δ_x along the x dimension, where

$$\Delta_x = \frac{\left[I(t,X) - I(t,X+a\hat{x})\right] + \left[I(t,X) - I(t,X-a\hat{x})\right]}{2} \qquad (16)$$

Similar averages along the N dimensions result in the approximation of the Laplacian in Eq. (14).

Remark 5 (Momentum term). The use of a nonzero DSR gain β results in a mass-like term in the approximation in Eq. (13). Therefore, the delayed reinforcement term $[I_i(k) - I_i(k-1)]$ in Eq. (11) is referred to as the momentum-term in search algorithms [17,18].

The proposed DSR-based information update in Eq. (11) captures a broad set of behaviors, as seen from the approximation by the damped-wave Eq. (13). For example, note that, as the DSR gain β increases from zero to one, the damping term $(1-\beta)$ in Eq. (13) tends to zero. Therefore, the overall behavior changes from overdamped (e.g., $\beta = 0$) to undamped ($\beta = 1$). For small DSR gain $\beta \to 0$, the DSR dynamics approximates the overdamped standard diffusion-type information transfer

$$\frac{\partial}{\partial t}I(t) = \gamma \frac{a^2}{2D}\nabla^2 I(t) \qquad (17)$$

With a larger DSR gain, $\beta \to 1$, the DSR dynamics approximates the superfluid-type information transfer, i.e.,

$$\frac{\partial^2}{\partial t^2}I(t) = \frac{\gamma a^2}{2D\delta_t}\nabla^2 I(t) = c^2 \nabla^2 I(t) \qquad (18)$$

where a smaller update-time interval δ_t (which is possible if the individuals can respond faster) leads to a larger speed of information propagation c.

2.5 Improvement in Performance With Delayed Self-Reinforcement. The DSR gain β should be selected to reduce the settling time of the system. Since the DSR gain β is a scalar parameter, numerical search methods could be used to optimally select it. Nevertheless, an analytical approximation-based approach, based on the continuous-time approximation of the discrete dynamics, is described below to select the DSR gain for the case when the eigenvalues of the matrix A are real. This approximation aids in understanding the potential settling-time improvement that can be anticipated with the proposed DSR method.

Similar to Eq. (6), and using arguments similar to the development of Eq. (13), the continuous-time version of the approximated dynamics with DSR in Eq. (11) is

$$\frac{d^2}{dt^2}I(t) + \frac{(1-\beta)}{\beta \delta_t}\frac{d}{dt}I(t) = -\frac{\gamma}{\beta \delta_t}AI(t) + \frac{\gamma}{\beta \delta_t}BI_s(t) \qquad (19)$$

where A is Hurwitz if the associated graph is connected as discussed in the paragraph after Eq. (6) in Sec. 2.2. Let the matrix A be similar to the matrix A_J in the Jordan form

$$A_J = T_A^{-1}AT_A \qquad (20)$$

where T_A is invertible, and the diagonal terms of the matrix A_J are the eigenvalues $\{\lambda_{A,i}\}_{i=1}^n$ of matrix A [33], which are assumed to

be real. Note that the multiplicity of each eigenvalue $\lambda_{A,i}$ can be more than one. With the transformation into modal coordinates

$$I(k) = T_A I_J(k) \qquad (21)$$

the network dynamics in Eq. (19) can be rewritten as

$$\frac{d^2}{dt^2}I_J(t) + \frac{(1-\beta)}{\beta\delta_t}\frac{d}{dt}I_J(t) = -\frac{\gamma}{\beta\delta_t}A_J I_J(t) + \frac{\gamma}{\beta\delta_t}B_J I_s(t) \qquad (22)$$

where $B_J = T_A^{-1}B$. Therefore, for each pole s_i of the approximate continuous-time dynamics in Eq. (6) without DSR, i.e.,

$$s_i + \gamma\lambda_{A,i} = 0 \qquad (23)$$

the corresponding poles of the approximate continuous-time dynamics in Eq. (22) with DSR are given by the roots of

$$s^2 + \frac{(1-\beta)}{\beta\delta_t}s + \frac{\gamma\lambda_{A,i}}{\beta\delta_t} = 0 \qquad (24)$$

or

$$s^2 + 2\zeta_i\omega_i s + \omega_i^2 = 0 \qquad (25)$$

where

$$\omega_i = \sqrt{\frac{\gamma\lambda_{A,i}}{\beta\delta_t}}, \quad 2\zeta_i\omega_i = \frac{(1-\beta)}{\beta\delta_t} \qquad (26)$$

Without DSR, let the settling time $T_{s,i}$ associated with eigenvalue $\lambda_{A,i}$ be estimated from Eq. (23) as a multiple of the time constant (the inverse of the distance of the eigenvalue from the imaginary axis in the complex plane when potential effects of eigenvalue multiplicity are neglected), e.g.,

$$T_{s,i} \approx \frac{4}{|s_i|} = \frac{4}{\gamma\lambda_{A,i}} \qquad (27)$$

Critical damping for the corresponding eigenvalue with DSR (corresponding to eigenvalue $\lambda_{K,i}$) occurs when damping $\zeta_i = 1$, i.e.,

$$\zeta_i = \frac{(1-\beta)}{2\beta\delta_t}\sqrt{\frac{\beta\delta_t}{\gamma\lambda_{A,i}}} = 1 \qquad (28)$$

with solution $\beta* < 1$ given by

$$\beta^* = (1 + 2\gamma\delta_t\lambda_{A,i}) - \sqrt{(1 + 2\gamma\delta_t\lambda_{A,i})^2 - 1} \qquad (29)$$

$$= \left(1 + \frac{8\delta_t}{T_{s,i}}\right) - \sqrt{\left(1 + \frac{8\delta_t}{T_{s,i}}\right)^2 - 1} \qquad (30)$$

Remark 6 (Reduction in settling time with DSR). Let pole s_i of the approximate continuous-time dynamics in Eq. (6) be the dominant dynamics (e.g., closest to the imaginary axis of the complex plane) without DSR. Then, the settling time $\hat{T}_{s,i}$ with DSR can be substantially smaller than the settling time $T_{s,i}$ without DSR, if the update time δ_t is small and if the settling time without DSR is large, i.e., $T_{s,i} \gg 1$, since for the critically damped case, the settling time $\hat{T}_{s,i}$ can be approximated, from Eqs. (26) and (27), as (again, potential effects of eigenvalue multiplicity are neglected)

$$\hat{T}_{s,i} \approx \frac{5.8}{\zeta_i\omega_i} = \frac{5.8}{\omega_i} = 5.8\sqrt{\frac{\beta^*\delta_t}{\gamma\lambda_{A,i}}} = 2.9\sqrt{\beta^*\delta_t T_{s,i}} \qquad (31)$$

3 Simulation Results and Discussion

Simulation results are presented to (i) evaluate the information transfer improvement with DSR when compared to the case without DSR; (ii) demonstrate that even second-order models cannot capture the superfluid-like information transfer without increasing the update rate when compared to the DSR-based model; and (iii) comparatively evaluate the impact on cohesiveness of swarming maneuvers with and without DSR.

3.1 Information Transfer Improvement With Delayed Self-Reinforcement. For a given system update-time interval δ_t, DSR can lead to substantial performance improvement when compared to the standard diffusive information transfer without the DSR. To illustrate this, the system used in simulations is composed of $n = 225$ individuals placed in a 15×15 regular array, where the spacing in the x and y directions was 1 m, as in Fig. 2. The neighborhood N_i of each individual was considered to be a disk of radius $r = 1.2$ m from the individual i. Thus, the average distance of individuals in the neighborhood was $a = 1$ m. The leader is the individual shown as a solid dot in Fig. 2.

In general, the information transfer improves when the alignment strength γ is increased. However, the maximum value of the alignment strength γ is bounded for a fixed update-time interval δ_t to ensure stability as in Eq. (9). In the following simulations, the update-time interval is kept fixed at $\delta_t = 0.01$. The initial values of the source information I_s and of all the individuals $I(0)$ were zero. The source information I_s is switched to one at the start of the simulations. With the alignment strength $\gamma = 100$ and without DSR, the settling time T_s needed for information I to reach and stay within $\pm 2\%$ of the final value of one, i.e., reach and remain between the horizontal black lines in Fig. 3, is 69 s. Moreover, without DSR, the information transfer becomes unstable as the alignment strength was increased to $\gamma = 101$ from $\gamma = 100$ as seen in Fig. 3. Therefore, the alignment strength γ was selected to be high ($\gamma = 100$) to enable a fast response, but kept smaller than the value $\gamma = 101$ that resulted in instability with the update-time interval $\delta_t = 0.01$ s.

The DSR gain β predicted to optimally improve the performance with DSR in Sec. 2.5 matches the results from a numerical search. The DSR gain β was varied and the resulting settling time T_s (i.e., the time needed for all the individual responses to come within and stay within 2% of the maximum value of the source information) is shown in Fig. 4. The settling time is minimized with the DSR gain $\beta = 0.96$. Note that the estimate of the optimal DSR gain β^* from Eq. (30) with the settling time from the case
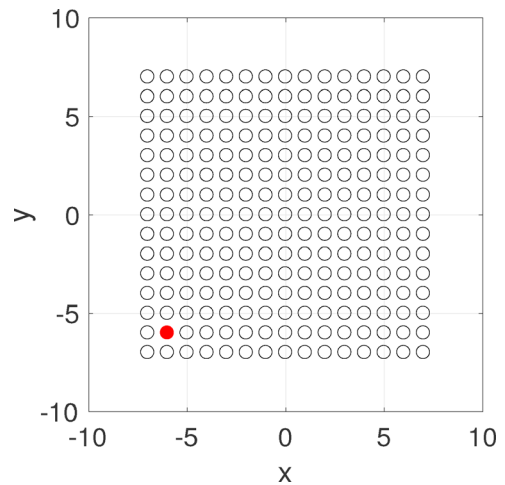

Fig. 2 The initial configuration of the 225 agents. Leader, represented by a solid dot, has access to the source information I_s from virtual agent s (not shown here).
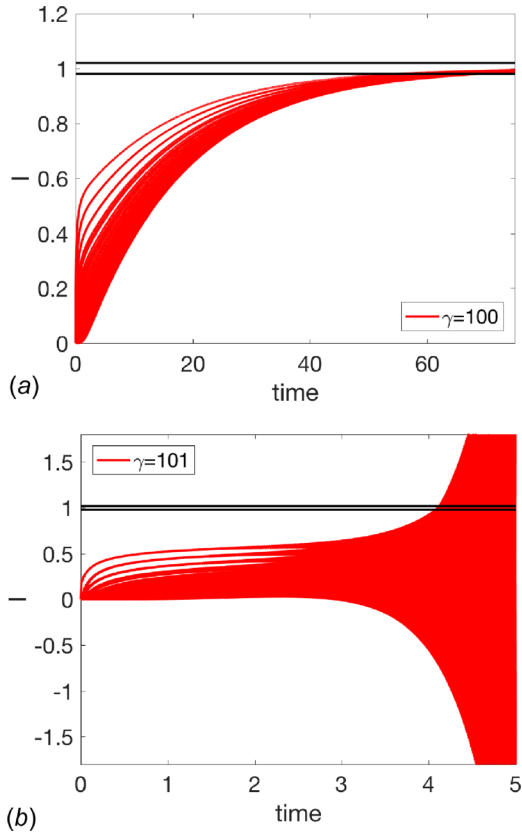
Fig. 3 Step responses without DSR for different alignment strength γ. The black lines show the $\pm 2\%$ deviation from the final value of one: (a) alignment strength $\gamma = 100$; the settling time is $T_s = 69\,\mathrm{s}$ and (b) alignment strength $\gamma = 101$; the response grows in an unbounded manner.
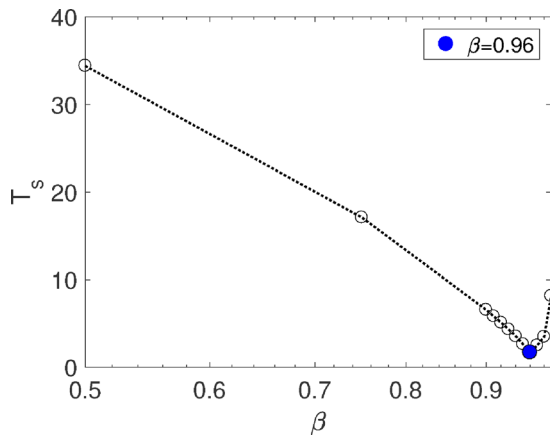

Fig. 4 Variation of settling time T_s for different DSR gains β

Fig. 5 Step responses with DSR for different gains β. The black lines show the $\pm 2\%$ deviation from the final value of one: (a) step response with optimal DSR gain of $\beta = 0.96$ with a settling time $T_s = 1.71\,\mathrm{s}$ and (b) a larger DSR gain $\beta = 0.98$ leads to oscillations and a larger settling time $T_s = 3.51\,\mathrm{s}$.

without DSR, i.e., $T_{s,i} = 69\,\mathrm{s}$ and the update-time interval $\delta_t = 0.01\,\mathrm{s}$ is 0.967, is close to the value of 0.96 obtained from the numerical search in Fig. 4.

The DSR gain β impacts the effective damping of the information-transfer dynamics. As the DSR gain β tends to one, the damping term $(1 - \beta)$ tends to zero and the overall behavior changes from overdamped, e.g., for DSR-gain $\beta = 0$ as seen in Fig. 3(a), to an oscillatory and underdamped response as seen in Fig. 5 for DSR-gain $\beta = 0.98$. Large oscillations can lead to distortions in the information transfer, and ideally, the DSR gain β should be tuned to be close to critical damping without too much overshoot. The minimal settling-time DSR gain of $\beta = 0.96$ yields
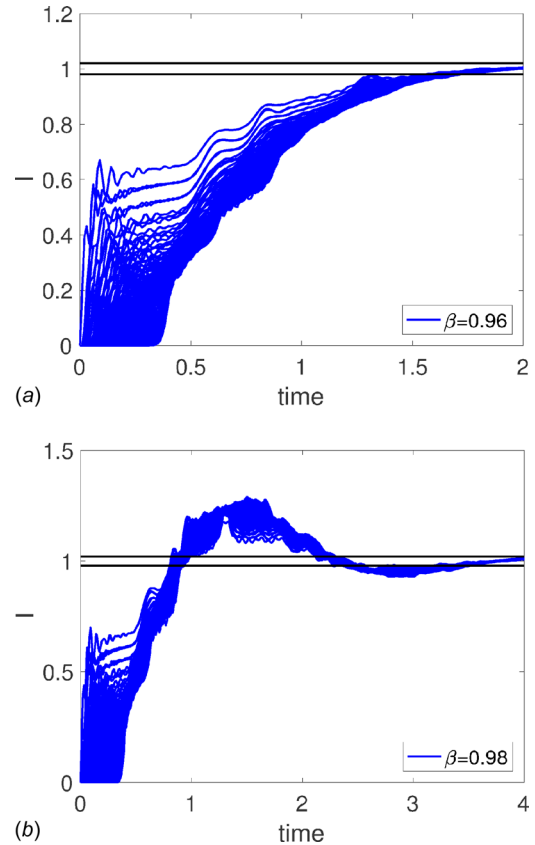
a fast response without noticeable overshoot as seen in the step response in Fig. 5(a).

The use of DSR leads to a substantial (more than an order) reduction in the settling time—from 69 s to 1.71 s, as seen by comparing the results in Figs. 3(a) and 5(a). Such improvement in the settling time with the DSR helps to increase the bandwidth of information that can be transferred without distortion. For example, with DSR, good tracking of information pulses can be expected provided the time period T_p of such pulses is greater than twice the settling time of $T_s = 1.71\,\mathrm{s}$. Without DSR, similar substantial improvements are not possible when the update-time interval is kept fixed at $\delta_t = 0.01\,\mathrm{s}$ since increases in the alignment strength lead to instability as seen in Fig. 3(b). Thus, for a given update rate δ_t, the proposed DSR leads to a more rapid transfer of information when compared to the case without the DSR.

3.2 Update-Rate for Faster Response Without Delayed Self-Reinforcement. Both the standard diffusive model in Eq. (1) and the second-order superfluid-type model in Eq. (13) can achieve faster information transfer, similar to the case with the use of DSR in Eq. (11), as shown in the simulation results in Fig. 6. Nevertheless, both these approaches require an increase in the update rate (i.e., smaller update-time interval δ_t) for such faster information transfer.

As seen in the simulation results in Fig. 6, the settling time with the standard diffusive model in Eq. (1) is 1.71 s (with the alignment strength γ increased about 40 times, from 100 to 4034) and with the superfluid-like model in Eq. (32) is 1.78 s, which are similar to the settling time of 1.71 s with the proposed DSR approach in Eq. (11). However, the standard diffusive model required a
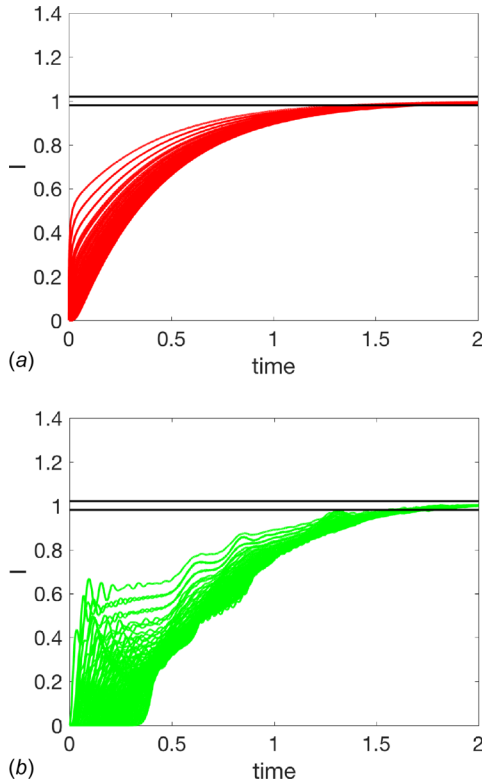
(a)

(b)

Fig. 6 Information transfer similar to the case with DSR in Fig. 5(a) with (a) standard diffusion model in Eq. (1) without DSR $\beta = 0$ but a larger alignment strength $\gamma = 4034$ and an update-time interval 2.48×10^{-4} s and (b) with the superfluid-type model in Eq. (32) and an update-time interval 1.24×10^{-4} s

(a)

(b)

Fig. 7 The time delay Δ_t between the leader and other individuals to reach 0.1 as a function of the distance d from the leader: (a) information transfer distance d is proportional to the square-root of time Δ_t with the standard diffusive model in Eq. (1) without DSR for individuals close to the leader and (b) linear with the DSR model in Eq. (11) and second-order superfluid-like model in Eq. (32)

proportional decrease in update-time interval by about 40 times, from 0.01 s to 2.48×10^{-4} s to maintain stability. The superfluid-like simulations were computed based on Eq. (13) as

$$I(k+1) = I(k) + \dot{I}(k)\hat{\delta}_t$$
$$\dot{I}(k+1) = \dot{I}(k) - \frac{(1-\beta)}{\beta\delta_t}\dot{I}(k)\hat{\delta}_t + \frac{\gamma}{\beta\delta_t}\Delta_i(k)\hat{\delta}_t \quad (32)$$

where the update-time interval was $\hat{\delta}_t$. With the same update-time interval of 2.48×10^{-4} s, the higher-order superfluid-like model was unstable, and hence, the results in Fig. 6(b) are shown with the update-time interval reduced, further, by half, i.e., to $\hat{\delta}_t = 1.24 \times 10^{-4}$ s.

To evaluate the information-transfer rate, the time delay Δ_t between the leader and other individuals to reach 0.1 is plotted as a function of the distance d from the leader in Fig. 7. Note that the information transfer distance is approximately linear in time Δ_t with the DSR, as seen in Fig. 7, for individuals close to the leader, which is expected for the relationship between the information-transfer distance d and time Δ_t for the superfluid-type model, e.g., see Ref. [9]. In contrast, the information transfer distance d is proportional to the square-root of time Δ_t with the standard diffusion model, as seen in Fig. 7(a), which is also as expected, e.g., see Ref. [9]. The speed of information transfer with DSR is also close to the expected value for the superfluid case, e.g., from the expression of c in Eq. (18). In particular, with an average distance of $a = 1$, for the two-dimensional case $D = 2$, alignment strength $\gamma = 100$ and update-time interval $\delta_t = 0.01$, the predicted speed c in Eq. (18) is $c = 50$ m/s. This is close to the speed of information transfer seen in the results in Fig. 7(b) for both, the second-order superfluid-type model and the proposed DSR approach. In particular, for the case with DSR, the information is transferred over a
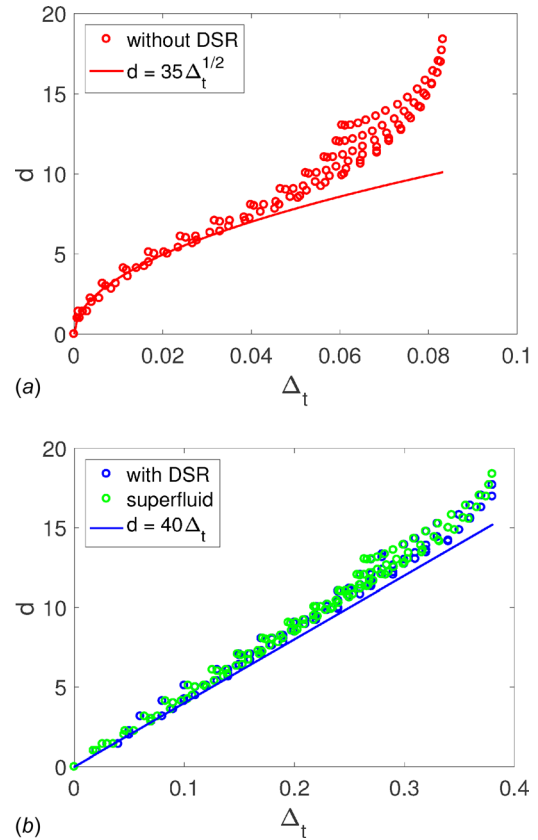
distance of 18.38 m in 0.38 s, i.e., at speed 48 m/s. Thus, the current superfluid-like model and standard diffusion models can only achieve the faster information transfer by increasing the individual, information-update rate. In contrast, the use of DSR achieves the superfluid-type information transfer and increases the overall information transfer rate in the network without requiring a corresponding increase in individual information-update rate.

3.3 Impact of Delayed Self-Reinforcement on Flocking. Delayed self-reinforcement can improve the cohesiveness of flocking maneuvers, when the orientation of each individual is considered to be the information I being transferred using local alignment to neighbors. It is noted that local alignment to neighbors cannot guarantee stability of the flock formation (with or without DSR). However, by improving cohesiveness, DSR improves the ability to maintain the formation. To illustrate, the position components x_i and y_i of each individual i are updated as

$$x_i(k+1) = x_i(k) + v\delta_t \cos I_i$$
$$y_i(k+1) = y_i(k) + v\delta_t \sin I_i \quad (33)$$

where v is the fixed speed of each individual and the information I_i is the orientation in the x–y plane. Second-order models have been used in flocking dynamics, e.g., see Ref. [11], however, such higher-order models also require an increase in update rate to achieve response rates achieved with the DSR approach as discussed in the last paragraph of Sec. 3.2. Note that the set of neighbors can change during these simulations, and control schemes
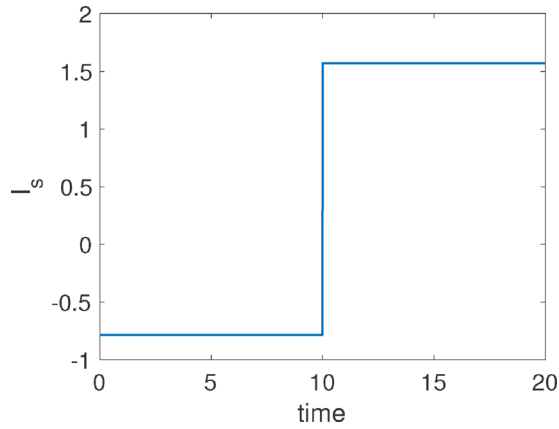
Fig. 8 The desired information source I_s, i.e., the orientation, is switched from $-\pi/4$ to $\pi/2$
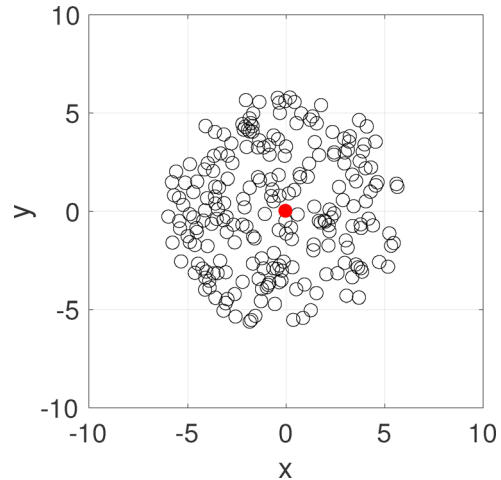

Fig. 9 The initial configuration of the 225 agents with random initial conditions. Leader, represented by a solid dot, has access to the source information I_s from virtual agent s (not shown here).

have been developed, e.g., to maintain spacing between individuals, e.g., see Refs. [7], [34], and [35]. Nevertheless, to focus on the impact of orientation-information transfer on the maneuver, effects such as speed changes or strategy changes to maintain spacing between individuals are not included in the simulations, as in other previous studies, e.g., see Refs. [4] and [9].

The use of DSR leads to improved cohesiveness in maneuvers when compared to the case without DSR, as illustrated below. The desired information source I_s (i.e., the desired orientation of the agents) is switched from an initial value of $-\pi/4$ that is held constant for 10 s and then switched to the final value of $\pi/2$, which is also then held constant for 10 s, as shown in Fig. 8.

Two cases, uniform and random initial distribution, of the agents are considered. For the random case, the initial locations were randomly chosen in a disk of radius $r_d = 6$, which was selected to be small enough to ensure that there was at least two individuals in each neighborhood N_i to facilitate connectivity of the overall network, which is needed for stability and cohesion as discussion in Sec. 2.2. The radial distance r_i from the center was chosen to be the square-root of a uniformly distributed random variable between 0 and r_d and the angle θ_i was selected to be a uniformly distributed random variable between 0 and 2π radians to yield the initial locations as $x_i = r_i \cos(\theta_i)$ and $y_i = r_i \sin(\theta_i)$. This square-root dependence on the radius results in a relatively uniform distribution over the area that depends on the square of the radius. Moreover, a uniformly distributed random noise $\hat{n}$ (between -0.025 rad and 0.025 rad) was added to the estimates of the averaged-neighbor orientation information update in Eq. (11) to yield

$$I_i(k+1) = I_i(k) - \gamma \Delta_i(k)\delta_t + \beta[I_i(k) - I_i(k-1)] + \hat{n} \quad (34)$$

and the resulting initial configuration is shown in Fig. 9.

The maneuver with DSR is more cohesive, for both uniform and random initial distribution, as seen in the similarity of the initial and final formations when compared to the case without the DSR. Even with the addition of noise in the information update for the case with random initial distribution, the overall motion remains cohesive, as seen by comparing the initial and final configurations of the agents, with and without DSR, in Fig. 10. Note that the turn movement (blue solid line) of the leader, in Fig. 10, is similar to that of an individual which is farther away, which is an important feature in biological flocks which exhibit equal-radius (parallel) trajectories [9]. In contrast, without DSR, the final direction of the leader (slope of the solid red line) is different from that of individuals farther away. Moreover, the slower transfer of turn-information leads to a larger turn radius without the DSR when compared to the case with the DSR, as seen in Fig. 10.

The radial acceleration of the agents during a turn has been used to investigate information transfer in biological swarms, e.g.,
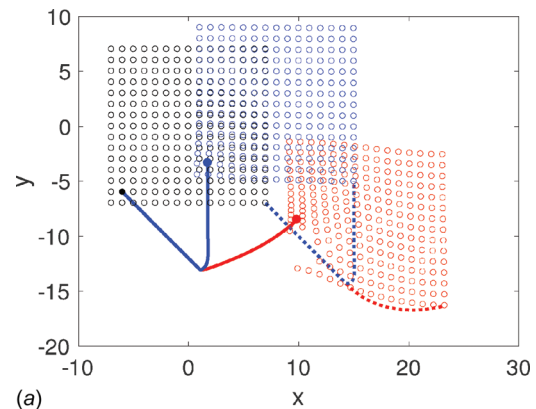
(a)
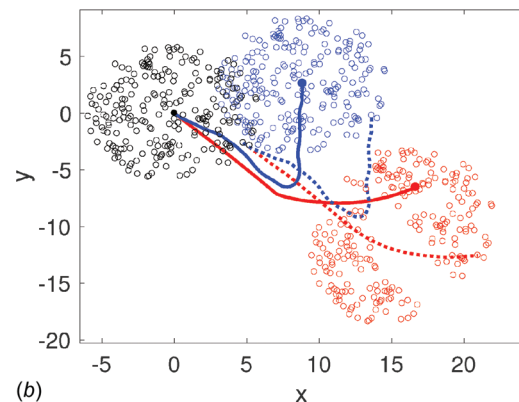
(b)

Fig. 10 Comparison of cohesiveness between the movement of the leader (solid line) and an individual farther away (dotted line); and the initial (black dots) and final formations (blue with DSR, red without DSR). The solid dot represents the leader, which has direct access to the information source I_s: (a) uniform initial spacing without noise in the updates and (b) random initial spacing in a circle with noise in the updates.

see Ref. [9]. In the noise-free, uniform-initial-conditions case, the radial acceleration a_r can be computed without the need for substantial filtering. For this case, the magnitude of the radial acceleration a_r does not reduce substantially with distance from the leader, as seen in Fig. 11(a). Such undamped transfer of radial acceleration across the network is considered to be a hallmark of
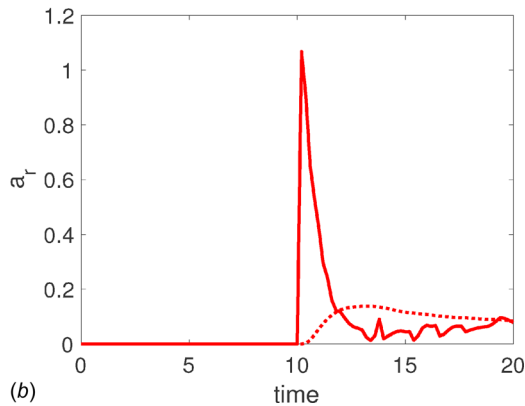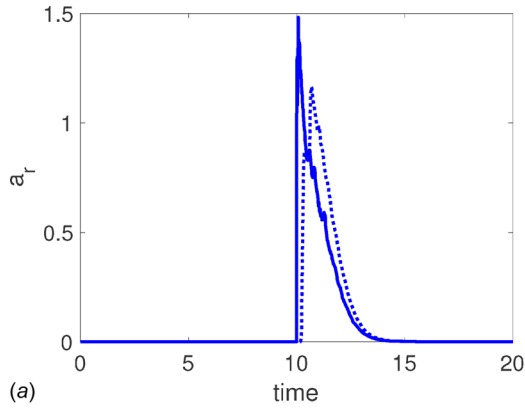
Fig. 11 The radial acceleration a_r of the leader (solid line) and individual farther away (dotted line) for the uniformly spaced initial conditions shown in Fig. 10: (*a*) with DSR and (*b*) without DSR

Fig. 12 Variation of distance d from the leader on the time-shift $\Delta_{t,c}$ needed to correlate the radial acceleration of each individual to that of the leader for the uniformly spaced initial conditions shown in Fig. 10: (*a*) with DSR and (*b*) without DSR

superfluid-like information transfer. In contrast, without DSR, the maximum value of the radial acceleration of the agent further away from the leader is substantially smaller than that of the leader, as seen in Fig. 11(*b*). This implies that the agent further away takes more time to accomplish a turn than the leader, which reduces the cohesion of the swarm during a maneuver without the DSR approach.

The time shift $\Delta_{t,c}$, needed for the individual radial acceleration to best correlate with the radial acceleration of the leader, varies linearly with distance d from the leader (for individuals close to the leader), with the DSR approach, as seen in Fig. 12(*a*). Based on this time-shift versus distance-to-leader, the overall speed of information transfer across the network is 48 m/s since the correlation time delay $\Delta_{t,c}$ is 0.38 s for a distance of 18.38 m. This is similar to the expected information transfer speed of 50 m/s based on the estimated value of c in Eq. (18) as described in Sec. 3.2. In contrast, without DSR, the speed of information transfer (based on the radial acceleration) is proportional to the square-root of the required time $\Delta_{t,c}$ as seen in Fig. 12(*b*), which is expected for diffusive information transfer. Both these features: (i) linearity of the information transfer with time and (ii) low distortion (dissipation free) transmission of information away from the leader, are indicative of superfluid-like flow of information observed in nature that cannot be explained by standard diffusion models [9].

Based on these results, the proposed DSR-based modification of the standard diffusion-based model captures the superfluid-like information transfer and the cohesiveness of turning maneuvers observed in natural swarms. Moreover, the proposed DSR-approach enables such improvements in information transfer without the need to increase the information update rate, i.e., bandwidth of each agent.
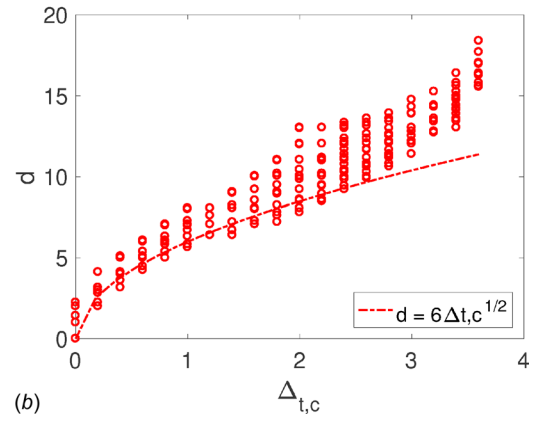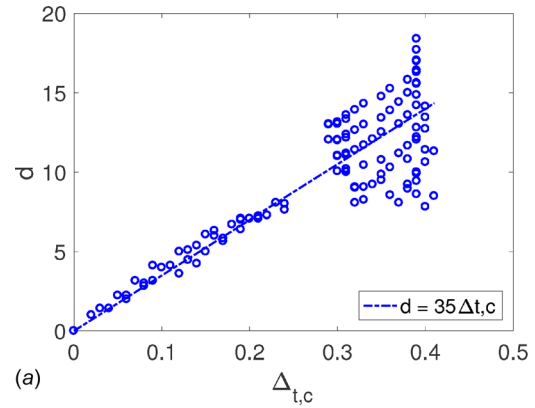
4 Conclusions

The speed of information transfer across the network impacts the cohesiveness and effectiveness of the network's response to external stimuli. However, as shown in the paper, the information transfer rate under the current diffusion-type models is bounded by the bandwidth (update rate) of each agent. To address this issue, the paper developed a new delayed self-reinforcement (DSR) approach to increase the information transfer rate without the need to increase the individual information-update rate. Example simulations showed substantial improvement, more than an order of magnitude increase, in the information transfer rate, with the DSR approach. Moreover, the DSR approach was shown to capture the superfluid-like, distortion-free information transfer observed in nature. Such rapid distortion-free information transfer with the DSR approach was then shown to enable maneuvers with (i) smaller turn radius and (ii) improved cohesiveness, both of which are important for the performance of natural and engineered swarms.

References

[1] Jadbabaie, A., Lin, J., and Morse, A. S., 2003, "Coordination of Groups of Mobile Autonomous Agents Using Nearest Neighbor Rules," IEEE Trans. Autom. Control, **48**(6), pp. 988–1001.

[2] Hedrick, J. K., Basso, B., Love, J., and Lavis, B. M., 2011, "Tools and Techniques for Mobile Sensor Network Control," ASME J. Dyn. Syst. Meas. Control, **133**(2), p. 024001.

[3] Huth, A., and Wissel, C., 1992, "The Simulation of the Movement of Fish Schools," J. Theor. Biol., **156**(3), pp. 365–385.

[4] Vicsek, T., Czirók, A., Ben-Jacob, E., Cohen, I., and Shochet, O., 1995, "Novel Type of Phase Transition in a System of Self-Driven Particles," Phys. Rev. Lett., **75**(6), pp. 1226–1229.

[5] Couzin, I., Krause, J., James, R., Ruxton, G., and Franks, N., 2002, "Collective Memory and Spatial Sorting in Animal Groups," J. Theor. Biol., **218**(1), pp. 1–11.

[6] Ren, W., and Beard, R. W., 2005, "Consensus Seeking in Multiagent Systems Under Dynamically Changing Interaction Topologies," IEEE Trans. Autom. Control, **50**(5), pp. 655–661.

[7] Olfati-Saber, R., 2006, "Flocking for Multi-Agent Dynamic Systems: Algorithms and Theory," IEEE Trans. Autom. Control, **51**(3), pp. 401–420.

[8] Bialek, W., Cavagna, A., Giardina, I., Mora, T., Silvestri, E., Viale, M., and Walczak, A. M., 2012, "Statistical Mechanics for Natural Flocks of Birds," Proc. Natl. Acad. Sci. U. S. A., **109**(13), pp. 4786–4791.

[9] Attanasi, A., Cavagna, A., Castello, L. D., Giardina, I., Grigera, T., Jelic, A., Melillo, S., Parisi, L., Pohl, O., Shen, E., and Viale, M., 2014, "Information Transfer and Behavioural Inertia in Starling Flocks," Nat. Phys., **10**(9), pp. 615–698.

[10] DeLellis, P., Porfiri, M., and Bollt, E. M., 2013, "Topological Analysis of Group Fragmentation in Multiagent Systems," Phys. Rev. E, **87**(2), p. 022818.

[11] Jahromi, H. T., and Haeri, M., 2013, "On Exponential Flocking to the Virtual Leader in Network of Agents With Double-Integrator Dynamics," ASME J. Dyn. Syst. Meas. Control, **135**(3), p. 034504.

[12] Boyd, S., Diaconis, P., and Xiao, L., 2004, "Fastest Mixing Markov Chain on a Graph," SIAM Rev., **46**(4), pp. 667–689.

[13] Wang, J., and Xin, M., 2013, "Flocking of Multi-Agent Systems Using a Unified Optimal Control Approach," ASME J. Dyn. Syst. Meas. Control, **135**(6), p. 061005.

[14] Carli, R., Fagnani, F., Speranzon, A., and Zampieri, S., 2008, "Communication Constraints in the Average Consensus Problem," Automatica, **44**(3), pp. 671–684.

[15] Atrianfar, H., and Haeri, M., 2013, "Theoretical Analysis of Flocking Algorithms in Networks of Second Order Dynamic Agents With Switching Topologies," ASME J. Dyn. Syst. Meas. Control, **136**(1), p. 011013.

[16] Fanti, M. P., Mangini, A. M., Mazzia, F., and Ukovich, W., 2015, "A New Class of Consensus Protocols for Agent Networks With Discrete Time Dynamics," Automatica, **54**, pp. 1–7.

[17] Rumelhart, D. E., Hinton, G. E., and Williams, R. J., 1986, "Learning Internal Representations by Error Propagation," *Parallel Distributed Processing*, Vol. 1, D. E. Rumelhart and J. L. McClelland, eds., MIT Press, Cambridge, MA, pp. 318–362.

[18] Qian, N., 1999, "On the Momentum Term in Gradient Descent Learning Algorithms," Neural Networks, **12**(1), pp. 145–151.

[19] Dohner, J., Eisler, G., Driessen, B., and Hurtado, J., 2004, "Cooperative Control of Vehicle Swarms for Acoustic Target Localization by Energy Flows," ASME J. Dyn. Syst. Meas. Control, **126**(4), pp. 891–895.

[20] Halloy, J., Sempo, G., Caprari, G., Rivault, C., Asadpour, M., Tache, F., Said, I., Durier, V., Canonge, S., Ame, J. M., Detrain, C., Correll, N., Martinoli, A., Mondada, F., Siegwart, R., and Deneubourg, J. L., 2007, "Social Integration of Robots Into Groups of Cockroaches to Control Self-Organized Choices," Science, **318**(5853), pp. 155–1158.

[21] Rubenstein, M., Cornejo, A., and Nagpal, R., 2014, "Programmable Self-Assembly in a Thousand-Robot Swarm," Science, **345**(6198), pp. 795–799.

[22] Olfati-Saber, R., Fax, J., and Murray, R., 2007, "Consensus and Cooperation in Networked Multi-Agent Systems," Proc. IEEE, **95**(1), pp. 215–233.

[23] Xi, J., Shi, Z., and Zhong, Y., 2012, "Consensus and Consensualization of High-Order Swarm Systems With Time Delays and External Disturbances," ASME J. Dyn. Syst. Meas. Control, **134**(4), p. 041011.

[24] Rastgoftar, H., and Jayasuriya, S., 2015, "Swarm Motion as Particles of a Continuum With Communication Delays," ASME J. Dyn. Syst. Meas. Control, **137**(11), p. 111008.

[25] Zhao, B., Lin, F., Wang, C., Zhang, X., Polis, M. P., and Wang, L. Y., 2017, "Supervisory Control of Networked Timed Discrete Event Systems and Its Applications to Power Distribution Networks," IEEE Trans. Control Network Syst., **4**(2), pp. 146–158.

[26] Xu, L., Xiao, N., and Xie, L., 2016, "Consensusability of Discrete-Time Linear Multi-Agent Systems Over Analog Fading Networks," Automatica, **71**, pp. 292–299.

[27] Meskin, N., and Khorasani, K., 2009, "Fault Detection and Isolation of Discrete-Time Markovian Jump Linear Systems With Application to a Network of Multi-Agent Systems Having Imperfect Communication Channels," Automatica, **45**(9), pp. 2032–2040.

[28] Nagarajan, H., Rathinam, S., and Darbha, S., 2015, "Synthesizing Robust Communication Networks for Unmanned Aerial Vehicles With Resource Constraints," ASME J. Dyn. Syst. Meas. Control, **137**(6), p. 061001.

[29] You, K., and Xie, L., 2011, "Network Topology and Communication Data Rate for Consensusability of Discrete-Time Multi-Agent Systems," IEEE Trans. Autom. Control, **56**(10), pp. 2262–2275.

[30] Cavagna, A., Del Castello, L., Giardina, I., Grigera, T., Jelic, A., Melillo, S., Mora, T., Parisi, L., Silvestri, E., Viale, M., and Walczak, A. M., 2015, "Flocking and Turning: A New Model for Self-Organized Collective Motion," J. Stat. Phys., **158**(3), pp. 601–627.

[31] Ballerini, M., Cabibbo, N., Candelier, R., Cavagna, A., Cisbani, E., Giardina, I., Lecomte, V., Orlandi, A., Parisi, G., Procaccini, A., Viale, M., and Zdravkovic, V., 2008, "Interaction Ruling Animal Collective Behavior Depends on Topological Rather Than Metric Distance: Evidence From a Field Study," Proc. Natl. Acad. Sci. U. S. A., **105**(4), pp. 1232–1237.

[32] Ren, W., 2007, "Multi-Vehicle Consensus With a Time-Varying Reference State," Syst. Control Lett., **56**(7–8), pp. 474–483.

[33] Ortega, J., 1987, *Matrix Theory, Classics in Applied Mathematics*, Vol. 3, Plenum Press, New York.

[34] Dohner, J., 1998, "A Guidance and Control Algorithm for Scent Tracking Micro-Robotic Vehicle Swarms," ASME J. Dyn. Syst. Meas. Control, **120**(3), pp. 353–359.

[35] Zhang, P., de Queiroz, M., and Cai, X., 2015, "Three-Dimensional Dynamic Formation Control of Multi-Agent Systems Using Rigid Graphs," ASME J. Dyn. Syst. Meas. Control, **137**(11), p. 111006.